Recrystallization texture in nickel heavily deformed by accumulative roll bonding

Mishin, O. V.; Zhang, Y. B.; Godfrey, A.

Published in:
I O P Conference Series: Materials Science and Engineering

Link to article, DOI:
10.1088/1757-899X/219/1/012034

Publication date:
2017

Document Version
Publisher's PDF, also known as Version of record

Recrystallization texture in nickel heavily deformed by accumulative roll bonding

IOP Conf. Series: Materials Science and Engineering **219** (2017) 012034 doi:10.1088/1757-899X/219/1/012034

Recrystallization texture in nickel heavily deformed by accumulative roll bonding

O V Mishin[1], Y B Zhang[1], and A Godfrey[2]

[1] Section for Materials Science and Advanced Characterization, Department of Wind Energy, Technical University of Denmark, Risø Campus, 4000 Roskilde, Denmark
[2] Key Laboratory of Advanced Materials (MOE), School of Materials Science and Engineering, Tsinghua University, Beijing 100084, China

E-mail: olmi@dtu.dk

Abstract. The recrystallization behavior of Ni processed by accumulative roll bonding to a total accumulated von Mises strain of 4.8 has been examined, and analyzed with respect to heterogeneity in the deformation microstructure. The regions near the bonding interface are found to be more refined and contain particle deformation zones around fragments of the steel wire brush used to prepare the surface for bonding. Sample-scale gradients are also observed, manifested as differences between the subsurface, intermediate and central layers, where the distributions of texture components are different. These heterogeneities affect the progress of recrystallization. While the subsurface and near-interface regions typically contain lower frequencies of cube-oriented grains than anywhere else in the sample, a strong cube texture forms in the sample during recrystallization, attributed to both a high nucleation rate and fast growth rate of cube-oriented grains. The observations highlight the sensitivity of recrystallization to heterogeneity in the deformation microstructure and demonstrate the importance of characterizing this heterogeneity over several length scales.

1. Introduction

Accumulative roll bonding (ARB) [1,2] is a severe plastic deformation technique, in which a single cycle consists typically of 50% rolling, cutting of the rolled material in half, cleaning and wire brushing of the surface, and then stacking the halves prior to repeating this process in subsequent cycles. This ARB process produces intrinsically heterogeneous microstructures as bonding interfaces are introduced during the multi-pass process. Regions near these interfaces have been found to be more refined than regions in between the interfaces [3–6], termed core regions in this work. In addition to these microscopic heterogeneities, the ARB process introduces severe sample-scale heterogeneities, which are reflected both in the through-thickness distribution of different texture components and also in the microstructure [3–10]. In recent publications on ARB-processed nickel, it has been shown that both microscopic and sample-scale heterogeneities have a significant influence on recrystallization [11,12]. Nevertheless, a strong cube texture has been observed in nickel processed by ARB to high strains [12]. In the present paper, formation of the cube texture is analyzed in nickel processed by ARB to a high von Mises strain, $\varepsilon_{vM} = 4.8$. Both the nucleation and growth of grains with different crystallographic orientations are characterized in this material, and the results are discussed in relation to the microstructural heterogeneities. The results are also compared to those obtained for nickel recrystallized after conventional rolling to similar strains.

2. Experimental

Strips of ~99.97% pure nickel with an average initial grain size of ~20 μm were deformed using a mineral oil as a lubricant [13]. The first 50% rolling pass was conducted on a strip with an initial thickness of 2 mm. The 1-mm thick sample was then cut in half, degreased and wire-brushed, after which the halves were stacked and rolled 50% again, creating a bonding between the two strips. After 6 passes, the total von Mises strain ε_{vM} was 4.8, and the sample consisted of 32 individual layers. The deformed material was then annealed in air at 220 °C for different periods of time.

Specimens from the longitudinal section containing the rolling direction (RD) and the normal direction (ND) were prepared for transmission electron microscopy (TEM) and scanning electron microscopy including electron backscatter diffraction (EBSD). A step size of 30 nm to 50 nm was used for a detailed analysis of deformed and recovered microstructures. Maps covering the entire sample thickness were obtained using a step size of 0.5 μm. For analysis purposes, the data set covering entire sample thickness was divided into two subsurface layers, two intermediate layers and one central layer, each with a thickness of 0.2 mm. The data obtained from the two opposite layers (either subsurface or intermediate) were averaged. Thus, only three distinct layers (subsurface, intermediate and central) are described in the following work.

Low angle boundaries (LABs) and high angle boundaries (HABs) were defined in the EBSD maps as those with misorientations θ between 2° and 15° and θ >15°, respectively. Recrystallized grains were defined as regions having a size of >3 μm with a misorientation angle of at least 1° (excluding twin misorientations). Three texture types were identified in the EBSD data: (i) the rolling texture, described as a combination of the Brass {110}⟨112⟩, S {123}⟨634⟩, Copper {112}⟨111⟩ and Dillamore {4 4 11}⟨11 11 8⟩ orientations; (ii) the shear texture, described as a combination of the {100}⟨011⟩, {111}⟨011⟩, {111}⟨112⟩, and {112}⟨110⟩ orientations; and (iii) the cube {001}⟨100⟩ texture.

3. Results

3.1. Deformed microstructure

The as-deformed microstructure is shown in figure 1(a), where it is apparent that regions within 50 μm to 80 μm from the immediate surface contain an increased frequency of the shear texture components. Orientations of the rolling texture dominate in the intermediate and center layers (figure 1(a) and table 1). A small frequency (~1%, see table 1) of cube-oriented lamellae and subgrains are present even in these layers. Considering the sample-scale heterogeneity, the subsurface contains the smallest fraction of the rolling texture components (f_{RoI}), and the smallest HAB spacing (d_{HAB}) along the ND (table 1). The difference in the average boundary spacing $d_{\theta>2^\circ}$ along the ND is however small, 155–160 nm.

The black elongated features in figure 1 correspond to fragments of the steel wire brush used for cleaning the surface before stacking and roll-bonding. These steel fragments are imprinted along the bonding interfaces (see figure 2). Statistical analysis has shown that the frequency of coarse (> 10 μm along the RD) steel fragments is higher along the interfaces created during the last two (the fifth and the sixth) passes [11]. The presence of these fragments results in formation of characteristic particle deformation zones (figure 2) similar to those previously observed around coarse particles in conventionally rolled materials [14,15]. Therefore, these fragments are also termed steel particles in the present work.

Table 1. Microstructural parameters and texture in the subsurface, intermediate, and central layers of the deformed material (data reproduced from [11] with permission of Springer).

Layer	f_{RoI} (%)	f_{Shear} (%)	f_{Cube} (%)	$d_{\theta>2^\circ}$ (nm)	d_{HAB} (nm)
Subsurface	48	17	1.7	160	285
Intermediate	82	2	1.1	156	310
Center	80	2	1.1	155	302

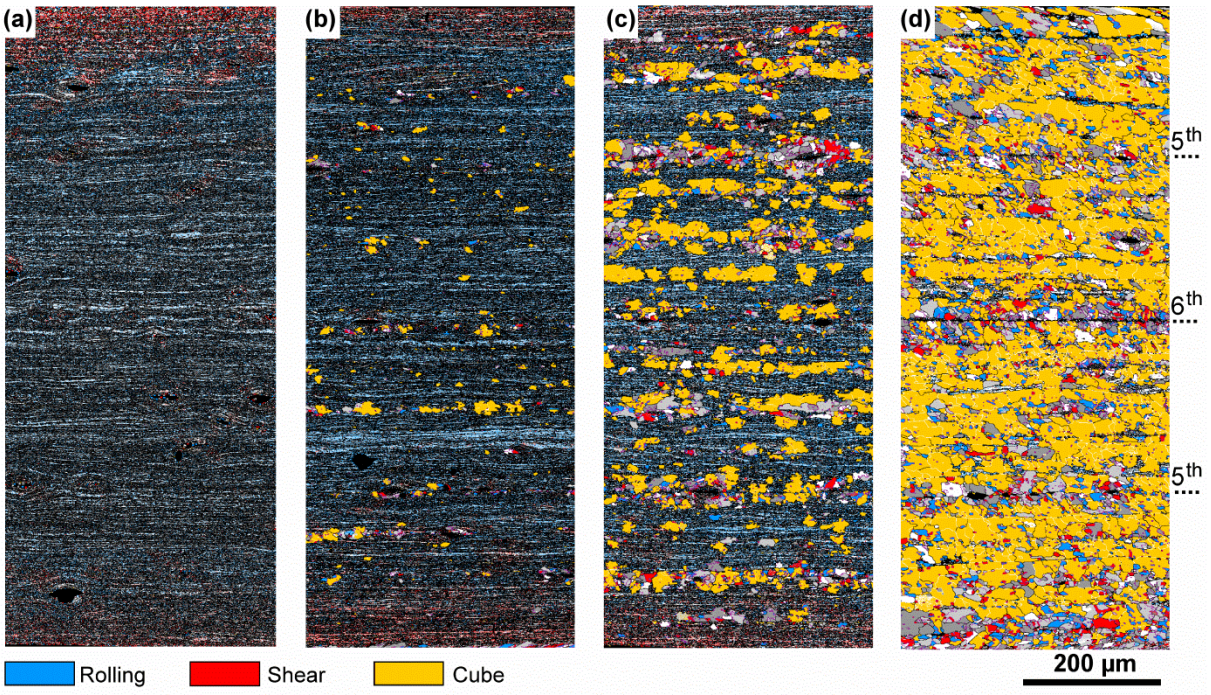

Figure 1. Orientation maps showing the microstructure over the entire thickness of the as-deformed sample (a) and of the samples annealed at 220 °C for 15 min (b); 30 min (c); and 90 min (d). The interfaces during the last two (the fifth and the sixth) rolling passes are indicted by the dashed lines on the right-hand side. LABs, HABs, and twin boundaries are shown as white, black and purple lines, respectively. The RD is parallel to the scale bar.

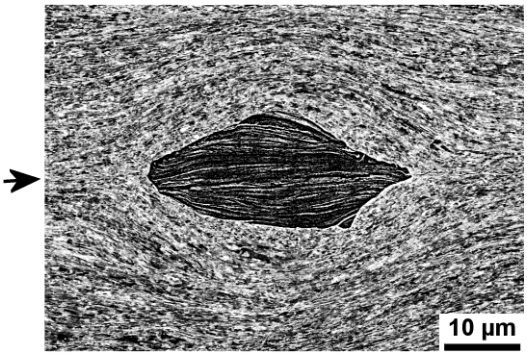

Figure 2. Backscatter electron image showing a particle deformation zone around a fragment of the steel wire brush used for cleaning the surface before stacking and roll-bonding. The arrow marks the position of a bonding interface.

3.2 Annealed microstructure

Annealing at 220 °C for 15 min results in the onset of recrystallization, with a large frequency of recrystallized grains nucleated near the bounding interfaces (typically at a distance of at least 1 µm from the closest interface), in particular, within particle deformation zones (figure 3). Other nucleation sites are shear bands and cube-oriented lamellae within the core regions. Many successful nuclei have orientations of the cube texture as seen in figure 1(b). In contrast, grains nucleated within the particle deformation zones and along the bonding interfaces formed during the last two rolling passes are characterized by a greater variety of orientations (figure 1(b) and 3(b)). The average size of recrystallized cube-oriented grains is 2 to 3 times greater than that for any other orientation class (see table 2). For each orientation class, the difference in the average grain size between the three layers is very small.

Table 2 also presents the nucleation rate, calculated as $N_v = N/(A\ d_{Rex+twins})$, separately for the different texture classes, where N is the number of recrystallized grains belonging to a certain texture class in an area A, and $d_{Rex+twins}$ is the average diameter of those grains, where twins are considered to be individual grains. It is seen that N_v for the cube-oriented grains in the subsurface is about one half of that in the other two layers. In each layer, the highest value of N_v is obtained for the rolling+shear texture, while the lowest value of N_v is recorded for the cube texture (see table 2). However, when the nucleation rate is normalized by the corresponding texture fraction in the as-deformed microstructure, a different situation emerges, where the normalized nucleation rate is the highest for the cube-oriented grains, and is lowest for the rolling+shear texture grains (table 2).

Table 2. Parameters characterizing the recrystallized grains, taking twins into account, in the ARB-processed Ni sample after 15 min at 220 °C. Here "roll+sh" correspond to regions of either the rolling or shear texture.

Layer	$d_{Rex+twins}$ (μm)			$N_v \times 10^{-3}$ (μm^{-3})			Normalized $N_v \times 10^{-3}$ (μm^{-3})		
	cube	roll+sh	other	cube	roll+sh	other	cube	roll+sh	other
Subsurface	5.5	2.1	3.0	0.08	0.57	0.43	5.0	0.8	1.9
Intermediate	5.7	2.1	2.9	0.15	0.75	0.57	13.8	0.9	3.8
Center	5.8	1.9	2.8	0.14	0.57	0.24	13.3	0.7	1.5

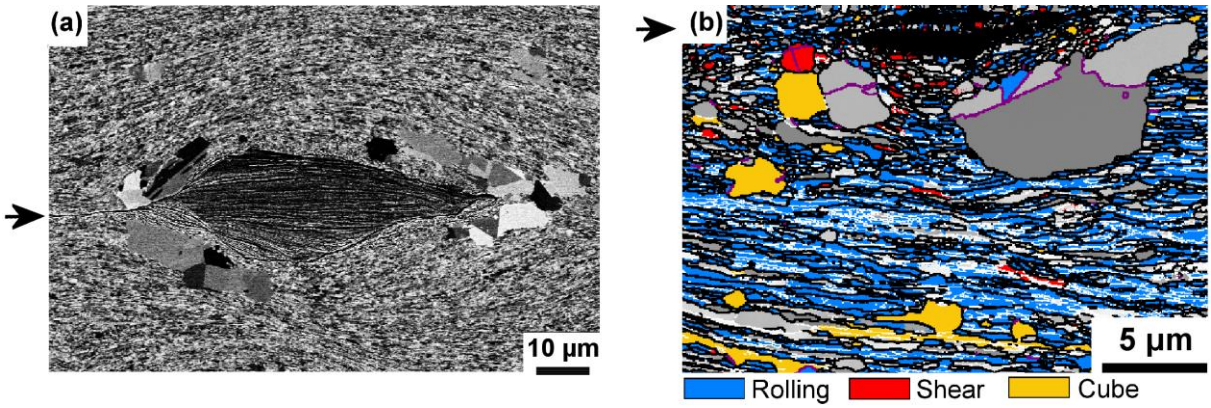

Figure 3. Examples of nucleation within particle deformation zones during 15 min of annealing at 220 °C: (a) backscatter electron image; (b) EBSD map, where LABs, HABs, and twin boundaries are shown as white, black and purple lines, respectively. Arrows mark bonding interfaces.

After 30 min of annealing the fraction recrystallized f_{Rex} is considerably higher in the intermediate layer than in the other layers (figure 4(a)). As f_{Rex} reaches at least 86% after 90 min of annealing, the difference in f_{Rex} between the layers becomes less significant. The average size of cube-oriented grains in each partially recrystallized condition is larger than that for any other orientation class (figure 4(b)), and the difference in $d_{Rex+twins}$ for the cube-oriented grains in the different layers remains small even in the almost fully recrystallized conditions. It is also noteworthy that grains with the rolling or shear texture have the smallest average size. There is also almost no difference in the evolution of texture between the intermediate and central layers. However, the subsurface layer contains consistently lower fractions of the cube texture, ending up with 55 % after 210 min of annealing, as compared to 66-69% in the other two layers (figure 5).

4. Discussion

ARB introduces both sample-scale and microscopic deformation heterogeneities arising directly from the nature of the process. The sample scale heterogeneities are similar to those produced by conventional rolling with large draughts [16,17] where a pronounced shear texture is developed near the surface of a rolled flat product. In ARB, after the cutting, wire brushing, and stacking process, some of this subsurface material is moved to the mid-thickness of the sample. The rolling texture in these regions after subsequent 50% is still slightly weaker than elsewhere, especially along the interfaces formed during the last two passes. Since these former subsurface regions experienced an additional shear deformation, the boundary spacing here is smaller, and hence the stored energy is higher than in the core regions. Additionally, coarse steel particles result in the development of particle deformation zones, which also contribute to a greater variety of orientations, a weaker rolling texture and a greater stored energy in the near-interface regions. The higher stored energy near the interfaces provides a higher driving force for recrystallization, which explains the high frequency of nuclei observed in the near-interface regions (figure 1(b–d)).

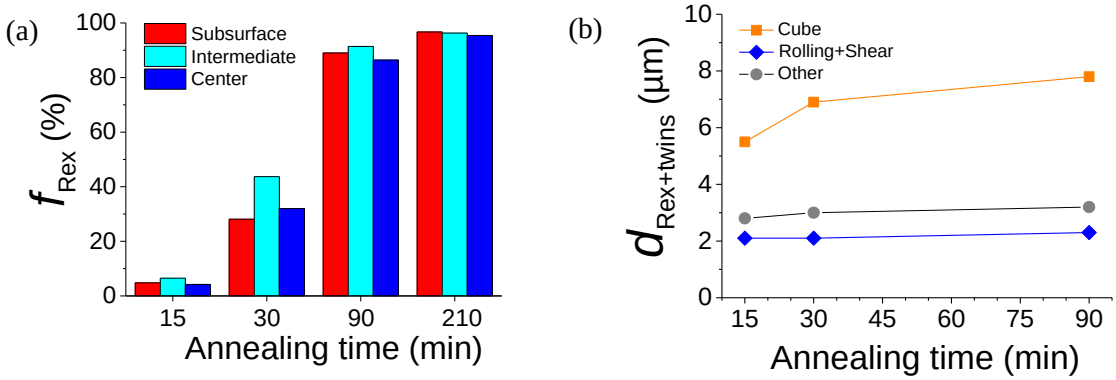

Figure 4. Parameters of recrystallized grains developed in ARB-processed Ni during annealing at 220 °C: (a) area fraction; (b) average sizes of grains calculated taking twin boundaries into account and covering the entire sample thickness.

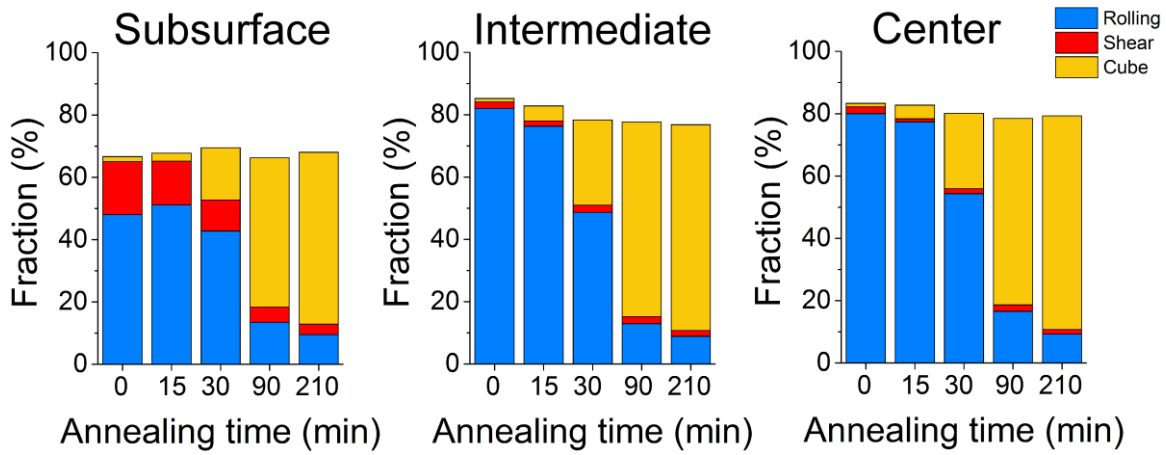

Figure 5. Fractions of different texture components in the three layers as a function of annealing time at 220 °C.

During recrystallization the cube grains quickly outgrow grains of other orientations, similar to the previous observations of conventionally rolled Ni [18, 19]. This growth advantage does not seem to be associated with the influence of impingement, as both cube and non-cube grains appear equally clustered (see figure 1(c)), though it is certainly only a qualitative assessment. A more detailed analysis based on

full determination of the Cahn-Hagel growth rates [20] for each orientation class is needed to confirm this.

Although recrystallization in the core regions, resulting in the strong cube texture, appears phenomenologically similar to that in conventionally rolled nickel [18,19], the presence of microscopic deformation heterogeneities in the form of interfaces with imprinted steel particles makes the annealing behavior and the recrystallized microstructure in the ARB-processed material rather unique. The microscopic heterogeneities produced by ARB are inherited in the recrystallized microstructure, where the near-interface regions typically contain lower frequencies of cube-oriented grains. This pattern has also been observed in Ni samples recrystallized after ARB to high and ultrahigh strains [12].

The sample scale deformation heterogeneities also affect the heterogeneity of the recrystallized microstructure. In the subsurface, the cube texture is consistently lower than in the other layers for each annealing duration (figure 5). The lower fraction of the cube texture in the subsurface is attributed to lower nucleation density of cube-oriented grains than in the other layers (see table 2), which is mainly because of the presence of the shear texture in the first 80 μm below the immediate surface, and hence a reduced rolling texture. It seems surprising that despite the reduced rolling texture, and therefore a smaller fraction of favorable misorientations between the cube-oriented grains and the recovered matrix in the subsurface [11], the cube-oriented grains here can grow to an average size similar to that in the other two layers. One possible reason is that the growth of a significant number of cube-oriented grains in each layer is confined by the bonding interface, so that the growth advantage of these grains in the rolling textured matrix, as typically seen in cold rolled nickel [18,19], is restricted along the ND.

5. Summary

The recrystallization behavior of Ni processed by accumulative roll bonding to a total accumulated von Mises strain of 4.8 has been examined, and analyzed with respect to heterogeneity in the deformation microstructure. It is found that the deformation microstructure near bonding interfaces is more refined and contains a higher stored energy compared to other regions. Particle deformation zones are also observed at bonding interfaces, resulting from embedded fragments of the steel wire brush used to prepare surfaces for the bonding process. The spatial arrangement of bonding interfaces produced during the ARB process consequently results in a sample-scale pattern of heterogeneity. In addition, a sample scale variation in local texture is also found, with distinct differences found in the subsurface, intermediate and center layers of the rolled material. The sample-scale and microscopic heterogeneities resulting from the ARB process are inherited in the recrystallized microstructure, where subsurface and near-interface regions typically contain lower frequencies of cube-oriented grains than anywhere else in the sample. Despite the microstructural heterogeneities, a strong cube texture forms in the sample after recrystallization, due to both the nucleation and growth advantage of cube-oriented grains. The complex pattern of heterogeneity developed during the ARB process, and the sensitivity of recrystallization to these variations, opens up the possibility for microstructural control in terms of both grain size and texture during thermomechanical processing, and highlights the importance of a thorough characterization of the deformation microstructure.

References

[1] Saito Y, Tsuji N, Utsunomiya H, Sakai T and Hong R G 1998 *Scr. Mater.* **39** 1221
[2] Saito Y, Utsunomiya H, Tsuji N and Sakai T 1999 *Acta Mater.* **47** 579
[3] Lee S H, Saito Y, Tsuji N, Utsunomiya H and Sakai T 2002 *Scr. Mater.* **46** 281
[4] Su L, Lu C, Li H, Deng G and Tieu K 2014 *Mater. Sci. Eng. A* **614** 148
[5] Najafzadeh N, Quadir M Z and Munroe P 2015 *Metall. Mater. Trans. A* **46** 4772
[6] Duan J Q, Quadir M Z and Ferry M 2016 *Metall. Mater. Trans. A* **47** 471
[7] Kim H W, Kang S B, Tsuji N and Minamino Y 2005 *Metall. Mater. Trans. A* **36** 3151
[8] Kamikawa N, Tsuji N, Huang X and Hansen N 2007 *Mater. Trans.* **48** 1978
[9] Li S, Sun F and Li H 2010 *Acta Mater.* **58** 1317
[10] Zhang Y B, Mishin O V and Godfrey A 2014 *J. Mater. Sci.* **49** 287

[11] Mishin O V, Zhang Y B and Godfrey A 2017 *J. Mater. Sci.* **52** 2730
[12] Zhang Y B and Mishin O V 2017 *Mater. Char.* **129** 323
[13] Zhang Y B, Mishin O V, Kamikawa N, Godfrey A, Liu W and Liu Q 2013 *Mater. Sci. Eng. A* **576** 160
[14] Humphreys F J 1977 *Acta Metall.* **25** 1323
[15] Mishin O V and Godfrey A, Juul Jensen D and Hansen N 2013 *Acta Mater.* **61** 5354
[16] Truszkowski W, Krol J and Major B 1980 *Metal. Trans. A* **11** 749
[17] Schoenfeld S E, Asaro R J 1996 *Int. J. Mech. Sci.* **38** 661
[18] Zhang Y B, Godfrey A, Juul Jensen D 2009 *Proc. 30th Risø Int. Symp. on Materials Science* (Roskilde, Denmark) ed. J C Grivel et al. pp 423
[19] Li X L, Liu W, Godfrey A, Juul Jensen D, Liu Q 2007 *Acta Mater.* **55** 3531
[20] Juul Jensen D 1992 *Scr. Mater.* **27** 533-538.